J Appl Physiol 99: 445–457, 2005.
First published November 19, 2004; doi:10.1152/japplphysiol.01144.2004.

Theoretical and empirical derivation of cardiovascular allometric relationships in children

Thierry Sluysmans[2] and Steven D. Colan[1]

[1]*Department of Cardiology, Children's Hospital, and the Department of Pediatrics, Harvard Medical School, Boston, Massachusetts and* [2]*Department of Pediatric Cardiology, Cliniques St Luc, Université Catholique de Louvain, Brussels, Belgium*

Submitted 11 October 2004; accepted in final form 17 November 2004

Sluysmans, Thierry, and Steven D. Colan. Theoretical and empirical derivation of cardiovascular allometric relationships in children. *J Appl Physiol* 99: 445–457, 2005. First published November 19, 2004; doi:10.1152/japplphysiol.01144.2004.—Basic fluid dynamic principles were used to derive a theoretical model of optimum cardiovascular allometry, the relationship between somatic and cardiovascular growth. The validity of the predicted models was then tested against the size of 22 cardiovascular structures measured echocardiographically in 496 normal children aged 1 day to 20 yr, including valves, pulmonary arteries, aorta and aortic branches, pulmonary veins, and left ventricular volume. Body surface area (BSA) was found to be a more important determinant of the size of each of the cardiovascular structures than age, height, or weight alone. The observed vascular and valvar dimensions were in agreement with values predicted from the theoretical models. Vascular and valve diameters related linearly to the square root of BSA, whereas valve and vascular areas related to BSA. The relationship between left ventricular volume and body size fit a complex model predicted by the nonlinear decrease of heart rate with growth. Overall, the relationship between cardiac output and body size is the fundamental driving factor in cardiovascular allometry.

heart size; cardiovascular growth; left ventricular volume

QUANTITATIVE ASSESSMENT OF cardiac and vascular dimensions is essential to evaluation and management of cardiovascular disorders (5, 6, 9, 42, 50, 54, 68, 71, 72). Critical to interpretation of these measurements is the establishment of normal standards. Despite the physiological and clinical importance of the issue, the best means by which to adjust for the impact of body size on the size of cardiovascular structures remains controversial. Numerous studies (14, 17, 24, 28, 31, 36, 50, 52, 55, 58, 68, 69) have addressed this issue but have reached different and therefore suspect conclusions. Nearly all have relied on simple regression analysis without a firm theoretical basis (1). Because intra- and interspecies studies have found body heat production and cardiac output (CO) to be linearly related to body surface area (BSA) over a broad range, the most commonly used method is a per-ratio standard approach, linearly adjusting cardiac and vascular dimensions to BSA. The critical test of whether this method fully accounts for the effect of body size has rarely if ever been applied; namely, the BSA-adjusted variables should have a distribution independent of body size. The fallacy of such "per-surface area standards" (75) has been amply demonstrated (21, 25, 28), but the correct method of adjusting for body size remains unclear.

This study reports the derivation of a theoretical, model-based prediction of the nature of the relationship between body size and the size of cardiovascular structures based on known control mechanisms, followed by empirical testing of the predictions in a large population of normal children aged 1 day to 20 yr old. Two primary assumptions underlie the formulation of the analysis: *1*) in nonstenotic vessels with normal flow velocity, volume of flow is assumed to be the primary determinate of vascular and valve size, and *2*) this relationship between flow and vessel caliber is assumed to result in a similar relationship between flow and orifice size in cardiovascular structures that carry a constant proportion of total CO. The basis for these assumptions is discussed, and their validity is examined relative to the measured data.

Glossary

2DEcho	Two-dimensional echocardiography
2DEDV	End-diastolic volume from two-dimensional echocardiography
AoIs	Aortic isthmus
AoRt	Aortic root
AVA	Aortic valve annulus
BSA	Body surface area
$BSA^{0.5}$	Square root of body surface area
BSA_{Bhw}	Body surface area calculated according to Boyd height and weight formula
BSA_{Bw}	Body surface area calculated according to Boyd weight formula
BSA_{D}	Body surface area calculated according to Du Bois and Du Bois formula
BSA_{H}	Body surface area calculated according to Haycock formula
BSA_{W}	Body surface area calculated according to Dreyer and Rey formula
CO	Cardiac output
EDD	Left ventricular end-diastolic diameter
EF	Ejection fraction
EDV	Left ventricular end-diastolic volume
HR	Heart rate
LLPV	Left lower pulmonary vein
LPA	Left pulmonary artery
LCA	Left carotid artery
LSCA	Left subclavian artery
LUPV	Left upper pulmonary vein

Address for reprint requests and other correspondence: S. D. Colan, Dept. of Cardiology, Children's Hospital, 300 Longwood Ave., Boston, MA 02115 (E-mail: colan@alum.mit.edu).

The costs of publication of this article were defrayed in part by the payment of page charges. The article must therefore be hereby marked "*advertisement*" in accordance with 18 U.S.C. Section 1734 solely to indicate this fact.

LVV	Left ventricular volume
$MMEDV_c$	End-diastolic volume from m-mode echocardiography, cubic formula
$MMEDV_{al}$	End-diastolic volume from m-mode echocardiography, area-length algorithm
MPA	Main pulmonary artery
MV_{AP}	Anteroposterior dimension of mitral valve
MV_L	Lateral dimension of mitral valve
MVA	Mitral valve area
PVA	Pulmonary annulus diameter
RPA	Right pulmonary artery
RLPV	Right lower pulmonary vein
RUPV	Right upper pulmonary vein
STJ	Aortic sinotubular junction
TPVCSA	Total pulmonary vein cross-sectional area
TrAo	Transverse aortic diameter
TV_{AP}	Anteroposterior dimension of tricuspid valve
TV_L	Lateral dimension of tricuspid valve
TVA	Tricuspid valve area

METHODS

Predictive model of optimum dimensions of the aorta and pulmonary artery. The optimum design of biological structures, evolved through the environmental pressure exerted by natural selection, is an established principle of biology that explains the curvilinear relation of the weight of a tree and the size of its branches (49), the relation between the diameters of pulmonary bronchi and bronchial air flow (30, 82), and the shape of eggs (78). There is a large body of evidence indicating that, under normal conditions, the geometry of the vascular pathways develops in a fashion that is optimal to minimize the hemodynamic cost of providing the volume of blood flow needed to support a wide range of body activities. For the vascular pathways, the operative physical principle is the need to minimize the energy required to propel blood through the vascular system by optimizing the interrelation between vessel radius and flow rates. This concept has been labeled the principle of minimum work. The energy required to propel flow is comprised of viscous and inertial forces. The viscous energy requirement relates to sheer stress (10, 85) and is inversely related to vessel radius. The inertial energy requirement is related to the oscillatory nature of blood flow, with the associated need to accelerate and decelerate flow with every beat, an energy requirement that varies directly with vessel radius. The dimension at which the sum of these two energy demands is minimized is the optimal vascular dimension (Fig. 1). The theoretical aspects and details of these calculations have been previously presented (56, 63, 66), and the theoretical foundations of the principle of minimum work (47, 48) and theoretical studies of optimality of the vascular system (20, 32, 33, 56, 67, 79, 86) have been validated for the coronary (66) and cerebral (63) arterial systems.

We calculated the aortic and pulmonary artery dimensions that theoretically minimize flow-related energy cost. The viscous and inertial energy requirements were calculated for the aorta and the main pulmonary artery (MPA) over the range of BSA from 0.2 to 1.8 m^2 and over the range of CO values corresponding to normal physical activities (from 3.5 to 17.5 $l \cdot min^{-1} \cdot m^{-2}$). Viscous energy loss per unit of length (E_V) was calculated by the Poiseuille equation, $E_V = (8q^2vl)/(\pi r^4)$, where q is the blood flow rate (cm^3/s), v is blood viscosity (0.03 $dyn \cdot s \cdot cm^{-2}$), r is the radius of the vessel, and l is the length of the vessel (56, 66). The inertial energy content (E_I) of blood volume was calculated as $E_I = b\pi r^2 l$, where r and l are as above and b is the energy coefficient of the blood volume (calculated in $dyn \cdot cm^{-2} \cdot s^{-1}$), obtained as the product of the mean arterial pressure times mean blood flow rate divided by the arterial vascular volume (66). Calculations assumed normal BSA-adjusted mean values of arterial pressure and CO and an arterial vascular volume of 4% of the total blood volume for the aorta and 0.7% for the MPA (45). The values for the energy coefficient b were similar to the values previously reported for coronary arteries (66). The optimum dimensions of the aorta and the MPA were then calculated as the dimensions for each that minimized the sum of E_V and E_I.

Predictive model of aortic branch size. Branching is an important feature of the vascular tree, which adds to the complexity of estimating optimal vessel size. In almost every part of the arterial tree, the area of the daughter branch is smaller than the area of the original vessel. In a constant-flow system, the velocity and energy expenditure increase exponentially as the diameter of the vessel decreases. If the same total flow is subdivided between two branch arteries of total cross-sectional area similar to the original vessel, the ratio of circumference to area rises, and more flow is exposed to the sheer stress of the vessel wall. Consequently, viscous forces are maintained at a similar level only if the sum of the daughter vessel areas is greater than that of the parent artery. In a pulsatile flow system, this must be balanced against the oscillatory energy cost of the system, which increases in proportion to the rise in cross-sectional area. The relation between the caliber of parent and branch vessels was originally described by Cecil D. Murray (47, 48) and further explored in later studies (20, 63, 67). The optimal model for the adaptation of the arterial tree is based on a balance between the radius of the vessel and

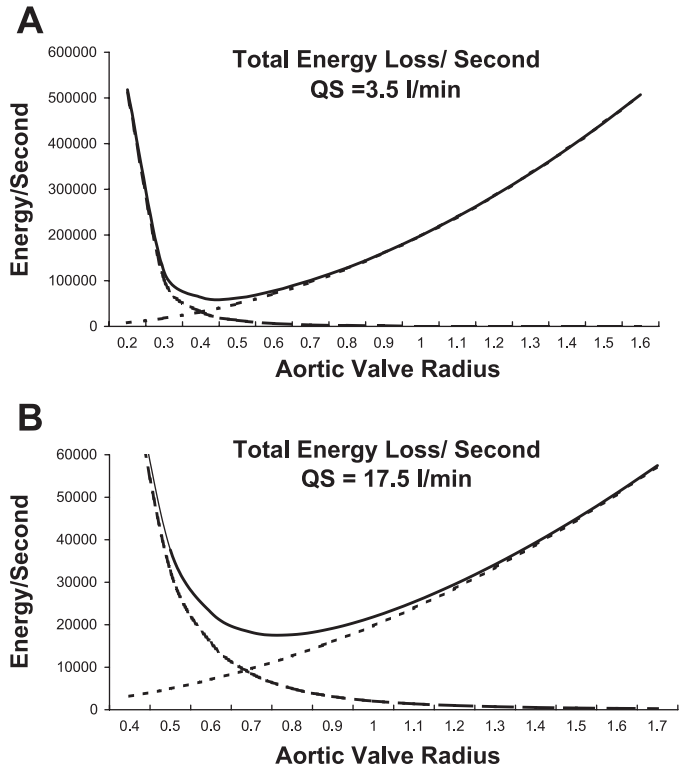

Fig. 1. Optimal aortic valve radius calculated according to the principle of minimal work for 2 levels of cardiac output. Energy loss per second (erg/s) because of viscous friction (dashed line) is plotted against the radius of the aortic valve (cm). On the same scale, the inertial energy content of blood (dashed-dotted line) and total energy loss calculated as the sum of viscous energy loss and inertial energy content loss (continuous thick line) are plotted for theoretical cardiac outputs (QS) of 3.5 l/min (*A*) and 17.5 l/min (*B*), representing the theoretical cardiac output at rest and at maximal exercise of a normal subject with a body surface area (BSA) of 1 m^2. The least amount of total energy loss per unit time corresponds to the minimum of the total energy loss curve. The corresponding radius for 3.5 l/min flow is 0.45 cm and 0.8 cm for 17.5 l/min. These values represent the theoretical range of normal optimal aortic valve radius for this BSA.

the cubic root of the flow through the vessel, such that the radii of parent (r_0) and branch (r_1, r_2, . . . r_n) vessels are related as ($r_0^x = r_1^x + r_2^x + \ldots + r_n^x$), where $x = 3$ for laminar flow and $x = 2.33$ for turbulent flow (56, 62, 63, 66, 67, 79). To verify whether the aortic branching system obeys this model for adaptation of the arterial tree in children, we examined the relation between the dimensions of transverse aorta and its branches over the range of BSA.

Testing of the model. The derived models were tested in a study group comprised of 496 normal children and young adults seen in the noninvasive laboratory at Boston Children's Hospital for echocardiographic evaluation during the years 1987 to 1998 who had no evidence of structural or functional heart disease. Acquired or congenital heart disease and other systemic disorders were excluded by a careful review of the medical history, electrocardiogram, chest X-ray, and echocardiogram. Specific exclusion criteria included acute or chronic systemic disorder, hypertension, a family history of hypertrophic or dilated cardiomyopathy, and height or weight percentile outside the range of normal. This study was conducted under a protocol approved by the Institutional Review Board in 1985.

Calculation of BSA. Height and weight were measured in the laboratory. To evaluate the potential differences between methods for calculating BSA, BSA was calculated according to five published methods.

The formula of Du Bois and Du Bois (16):

$$BSA_D = height^{0.725} \cdot weight^{0.425} \cdot 0.007184 \quad (1)$$

The method of Dreyer and Ray (15):

$$BSA_W = weight^{0.6666} \cdot 0.1 \quad (2)$$

The two methods published by Boyd (7):

$$BSA_{Bw} = 0.0004688 \cdot (1{,}000 \cdot weight)^{0.8168 - 0.0154 \log(1{,}000 \cdot weight)} \quad (3)$$

$$BSA_{Bhw} = 0.0003207 \cdot (1{,}000 \cdot weight)^{0.7285 - 0.0188 \log(1{,}000 \cdot weight)} \cdot height^{0.3} \quad (4)$$

The formula of Haycock et al. (27):

$$BSA_H = height^{0.3964} \cdot weight^{0.5378 \cdot 0.024265} \quad (5)$$

Data collection. Echocardiographic studies were performed with a phased-array sector scanner (Hewlett-Packard or Acuson) equipped with transducers appropriate for body size and were recorded on 0.5-in. videotape cassette at 30 frames/s. Subxiphoid, apical, parasternal long and short axis, and suprasternal notch views were obtained for each patient. When necessary, subjects less than 2 yr of age were sedated with chloral hydrate. All measurements were performed by one of two observers. Measurements were performed either online during the exam or secondarily offline from videotape. Online measurements were performed from video loops captured in zoom mode by use of the electronic calipers on the ultrasound machine. Offline measurement was performed either using electronic calipers on a video overlay system or from video page prints using a digitizing tablet. All valvar and vascular dimensions were measured from inner surface to inner surface at the moment of maximal expansion during the cardiac cycle. The dimensions of the aortic valve annulus (AVA), aortic root (AoRt), and sinotubular junction (STJ) were measured on parasternal long axis views (61). The measurements of the transverse aorta (TrAo), left subclavian (LSCA), and left carotid arteries (LCA) at their origin and of the aortic isthmus (AoIs) were obtained from high parasternal long axis or suprasternal notch views (26, 73). The lateral dimensions of mitral and tricuspid valves were measured on four chamber apical views (MV_L and TV_L, respectively) and the anteroposterior dimension from the left parasternal long axis view (MV_{AP} and TV_{AP}, respectively) at the proximal attachment of the leaflets at each side of the annulus (26, 34). The mitral and tricuspid valve areas (MVA, TVA) were calculated as an ellipse [$\pi \cdot (d_1/2) \cdot (d_2/2)$, where d_1 and d_2 are the anteroposterior and lateral dimensions, respectively] in those subjects for whom both measurements were available. The dimensions of the pulmonary valve annulus (PVA), the MPA, and the proximal right and left pulmonary arteries (RPA, LPA) were measured from left parasternal, short axis views. The pulmonary veins were measured from subcostal, apical, high parasternal, or suprasternal notch short axis views at the point of connection to the left atrium. Total pulmonary venous cross-sectional area (TPVCSA) was calculated as the sum of the cross-sectional areas of the four individual pulmonary veins. Two-dimensional end-diastolic volume (2DEDV) was calculated from long and short axis views of the left ventricle obtained from apical and parasternal windows, respectively. Diastolic images were taken as the frame preceding mitral valve closure, and the endocardial and epicardial volumes were calculated by the biplane Simpson's algorithm (84).

Previously published (11) left ventricular end-diastolic short axis dimensions (EDD) obtained from digitized m-mode recordings in 290 normal children aged 0 to 18 yr were reanalyzed to obtain measurements of end-diastolic volumes by use of other algorithms, permitting us to examine the impact of the method of calculating end-diastolic volume on the relationship to body size. Heart rate was calculated from the R-R interval on the electrocardiogram. M-mode-derived left ventricular end-diastolic volume (MMEDV) was calculated by two methods. For all 290 subjects, cubic-formula end-diastolic volume ($MMEDV_c$) was estimated as the cube of the short axis dimension = EDD^3. For those subjects in whom left ventricular long axis dimensions could be measured ($n = 176$ of 290), area-length end-diastolic volume ($MMEDV_{al}$) was also estimated by using the 5/6·area·length algorithm. The two-dimensional (2DEDV) and m-mode ($MMEDV_c$, $MMEDV_{al}$) volume measurements represent independent data sets and were therefore analyzed separately.

Statistical analyses. Linear, nonlinear, and multiple regression analyses were used to examine the relationship between parameters of body size and each of the echocardiographic variables. On the basis of preliminary exploratory analysis and theoretical considerations as discussed above, an exponential growth model with a zero intercept ($Y = aX^b$, where Y = cardiovascular dimension and X = body size parameter) was used to test the relation of echocardiographic measurements to body height, body weight, and BSA calculated according to the five methods described above. Three-parameter models of the form $Y = aX^b + c$ were examined to determine whether a statistically significantly improved [$P < 0.05$ by F-statistic as described by Zar (87)] description of the relationship between body size and echocardiographic measurements could be achieved through the use of higher order models. Nonlinear curve fits were calculated by the Levenberg-Marquardt least-square method (41). The model with the highest R value and the lowest residual mean square and the lowest square root of residual mean square (= standard error of the estimate) was considered to provide the "best fit." After derivation of the exponents for the exponential growth model, the significance of the difference between the derived and the theoretically predicted exponents was tested. Proceeding from the assumption that the control mechanisms for vascular growth should be uniform across the vascular and valve structures included in the analysis, we further evaluated the theoretical model based on whether a similar trend was observed for most or all of the variables. To test for the absence of heteroscedasticity and skewness in prediction (1) after transformation of valvar and vascular measured dimensions by division (index = dimension/square root of BSA_H, where BSA_H is BSA derived from the Haycock formula) the relations between body size and the indexed variables were tested for skewness and were analyzed by regression analysis for linear trends.

RESULTS

Prediction of optimum vascular dimensions on the basis of the principle of minimum work. Observed diameters of aortic valve, ascending aorta, pulmonary valve, and central pulmonary artery were compared with the values predicted by the

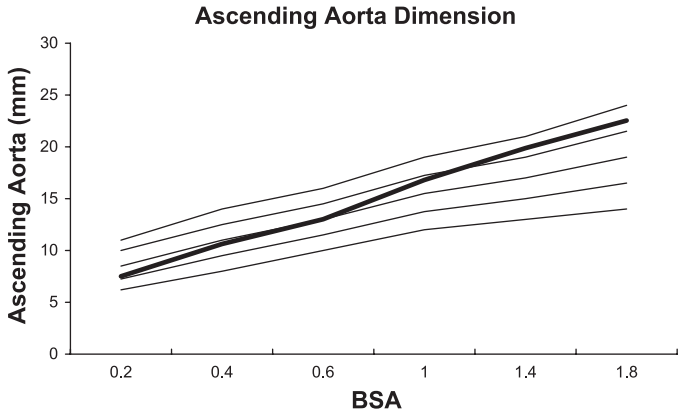

Fig. 2. Principle of minimum work: comparison of optimal dimensions and observed dimensions of vascular pathways. Comparison of the optimal valve and vascular diameters derived from the theoretical principle of minimal work and calculated for cardiac output of 1 × 3.5 l/min, 2 × 3.5 l/min, 3 × 3.5 l/min, 4 × 3.5 l/min, and 5 × 3.5 l/min, respectively (thin lines, from low to high values) with the mean observed values (thick line) of the ascending aorta in normal subjects. The normal mean diameters are optimal in terms of energy dissipation for cardiac output equivalent to 2 times the cardiac output at rest in infants and ~4 times the cardiac output at rest for older children, corresponding to the progressively higher peak activity level and heart rate reserve associated with growth. Vascular dimensions appear optimized to accommodate the cardiac output associated with peak normal activity.

principle of minimum energy dissipation over the entire range of body size (0.2–1.8 m^2 BSA).

Optimal aortic dimensions calculated according to the principle of minimal work are presented for CO ranging from normal resting levels (3.5 $l \cdot min^{-1} \cdot m^{-2}$) to CO associated with maximal activity (5 × 3.5 $l \cdot min^{-1} \cdot m^{-2}$) in Fig. 2. The observed diameters were found to be optimal in terms of energy dissipation for CO up to two times the resting CO in infants, increasing to values that were optimal for three to four times the resting CO for older children. Data obtained from athletes and hypertensive subjects indicate that cardiac structures adapt to peak or mean 24-h levels of pressure and volume demand (8, 12, 18, 19, 43, 65). Heart rate response is the primary determinant of CO increase with exertion, and infants have an approximate twofold magnitude of heart rate reserve, a value that increases to three- to fourfold in older children and young adults. Thus the difference between observed diameters that are optimal in terms of energy dissipation in infants vs. children corresponds to the expected difference in CO associated with age-appropriate physical activity and range of intensity of exertion.

Predictive model of aortic branch size. The calibers of the transverse aorta and branch vessels (LCA, LSCA, and AoIs) were found to be related according to $r_0^x = r_1^x + r_2^x + r_3^x$ with $x = 2.33$, as demonstrated by linear regression and by calculation of the indexed mean values of the radii (Fig. 3). The value $x = 2.33$ is the value expected for an optimal relation between the calibers of parent and daughter vessels in turbulent flow (56). Curves, branches, and projections impose directional change on the flow streamlines, resulting in nonlaminar flow in the horizontal aorta and its branches (4, 40, 44). Over the range of body size, the observed relation between the dimensions of the transverse aorta and its branches were therefore found to conform to the theoretical principle of optimum dimension relation.

Comparison of methods for calculating BSA. The relationship between BSA_H vs. each of the other four methods of calculating BSA is illustrated in Fig. 4. It has been previously documented that the formula of Du Bois and Du Bois increasingly underestimates (27) BSA as values fall below 0.7 m^2, an observation confirmed in these data. BSA calculated according to each of the other three formulas demonstrated significantly skewed comparison at lower compared with higher BSA values, although for each of the other methods lower values of BSA were overestimated compared with the Haycock formula. For each of the cardiovascular parameters examined in this study, BSA_H was more closely correlated than any of the other four formulas (data not shown). For these reasons, BSA_H was considered the most appropriate method for calculating BSA, and only analyses based on BSA_H are presented.

Relation of valvar and vascular dimensions and areas to body size. The range, the number of observations, the mean and the median values of cardiac, valvar and vascular diameters, areas, and volumes are reported along with descriptive statistics for age, height, weight, and BSA in Table 1. For each of the valvar and vascular diameters, indexing to BSA_H failed to adequately account for the variance with BSA. Because the results of this analysis were similar for all 19 variables, the details of this analysis are illustrated only for the AVA (Fig. 5). In Fig. 5*A*, the close linear relationship between AVA and BSA_H is apparent. Nevertheless, when AVA is "indexed" by simple division by BSA, AVA/BSA is found to be strongly inversely and nonlinearly dependent on BSA, as shown in Fig. 5*B*. Thus this method of adjusting for body size fails to fully account for the dependence of AVA on BSA. This approach to normalization failed in a similar fashion for all 19 variables. The principle of minimal work predicts a linear relation between vessel cross-sectional area and the volume of flow through the vessel. For the cardiac valves and central vessels, the volume of flow is either total CO or a fixed proportion thereof. Therefore, their area should relate to BSA and their

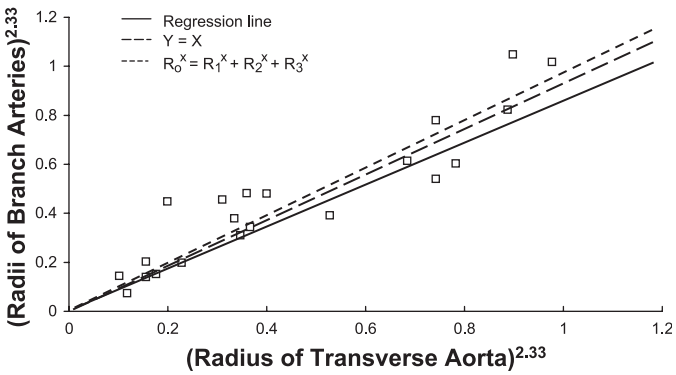

Fig. 3. Relation of the radius of the transverse aorta to the sum of its branches. The *x*-axis is (radius of transverse aorta)$^{2.33}$, and the *y*-axis is (radius left carotid)$^{2.33}$ + (radius left subclavian artery)$^{2.33}$ + (radius aortic isthmus)$^{2.33}$. The calibers of the transverse aorta and its branch vessels are related according to $r_0^x = r_1^x + r_2^x + \cdots + r_n^x$, with $x = 2.33$, as demonstrated by linear regression and by calculation with the indexed mean values of the radii ($1.53^{2.33} = 1.13^{2.33} + 0.64^{2.33} + 0.58^{2.33}$, indexed values from Table 2). The line of identity ($X = Y$) is shown to illustrate that both the theoretically predicted relationship and the regression line are insignificantly different from the line of identity. Over the range of body size, the observed relation between the dimension of transverse aorta and its branches follows the theoretical principle of optimum dimension relation.

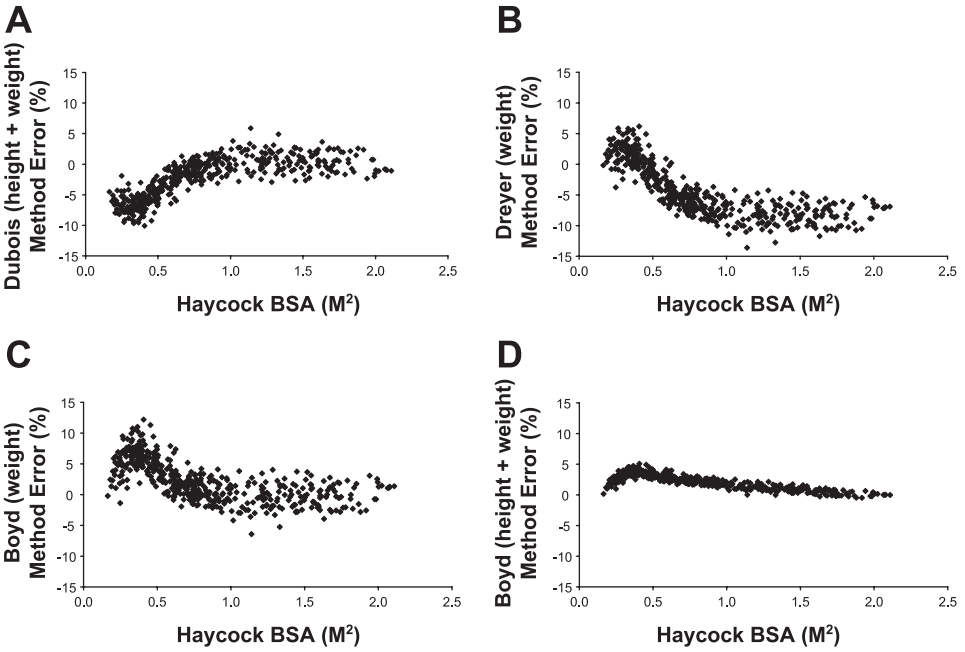

Fig. 4. Comparison of methods for calculating BSA. Each graph displays the percent difference between BSA calculated according to the Haycock formula (27) (Haycock BSA) and BSA calculated by the method indicated on the *y*-axis, plotted against Haycock BSA. Dubois [height + weight (H+W)] method (*A*) is the formula of Du Bois and Du Bois (16). Dreyer (W) method (*B*) is the method of Dreyer and Rey (15). Boyd (W) method (*C*) is the formula of Boyd (7) calculating BSA from weight alone. Boyd (H+W) method (*D*) is the formula of Boyd (7) calculating BSA from height and weight. Each method shows a different pattern of skewed errors with differences as great as 10% for all but Boyd (H+W).

diameter should be proportional to $BSA^{0.5}$. Although the regression of AVA vs. $BSA^{0.5}$ is only marginally better than the regression vs. BSA (Fig. 5*C*), when AVA is indexed by division by $BSA^{0.5}$, $AVA/BSA^{0.5}$ is found to manifest no significant residual dependence on BSA, as shown in Fig. 5*D*. Figure 5 also illustrates the problem of nonconstant variance (heteroscedasticity) because there appears to be a larger data spread in AVA for higher values of BSA and larger spread of indexed AVA for lower values of BSA. However, this degree of skewness in the residuals was not statistically significant, as discussed below.

We next evaluated whether the mathematical relation between observed vessel and valve diameter and body size was significantly different from the theoretical prediction. We examined whether height, weight, or BSA_H provided a better means of accounting for the variance in the valvar and vascular diameters. Comparisons of the relationship between each of the valvar and vascular diameters vs. height, weight, and BSA_H are presented in Table 2. For each regression, the constant (*a*) and exponent (*b*) fit to a function of the form $Y = aX^b$ are shown, with the correlation coefficient and the residual mean square. In each instance, the correlation coefficient was larger and the residual mean square was lower for the regression against BSA_H. Three parameter models of the form $Y = aX^b + c$ were also examined for each variable. In each instance, the addition of the third parameter did not significantly improve the accuracy of the prediction of the *Y* values, justifying reliance on the simpler two-parameter model.

Comparison of the exponents in the regressions across variables in Table 2 indicated that vascular and valvar dimensions correlated on average with BSA_H raised to the 0.50 power (range 0.42 to 0.58). On the basis of the observations that *1*) all valve and vascular dimensions related more closely to BSA_H than to height, weight, or BSA calculated by other methods, *2*) on average valve and vascular diameters relate most closely to $BSA_H^{0.5}$, and *3*) each of the valvar and vascular diameters carry either the total or a constant proportion of CO and should therefore demonstrate a similar exponential dependence on BSA_H, we next examined whether the derived exponent for any of these variables vs. BSA_H was significantly different from the average exponent of 0.5. Table 2 presents the results for the linear regressions of each of the valvar and vascular diameters to functions of the form $Y = a(BSA_H)^{0.5}$ and of the form $Y = a(BSA_H)^{0.5} + c$. For each of the parameters, there was no significant change in residual mean square compared with the more general $Y = aX^b$ model (Table 2), indicating that the simpler linear model using $(BSA_H)^{0.5}$ as the independent variable was equally successful in describing the relationship between BSA and the size of vessels and valves.

When we evaluated whether the inclusion of a nonzero intercept in the linear model significantly improved the explained variance, the only variables for which the intercept was distant more than 1 mm from 0 were mitral and tricuspid annulus diameters and pulmonary venous diameters. For each of these, the *P* values for the intercept were less than 0.10. To determine whether these significant intercept *P* values related to age-related differences in the shape of the atrioventricular valves or relative size of individual pulmonary vein diameters, we analyzed the relationship of MVA, TVA, and TPVCSA to BSA. The analysis for these variables, conducted in a fashion similar to that for the diameters, is presented in Table 3. As predicted, the areas related more closely to BSA_H than to height or weight, and the exponent *b* of the $Y = aX^b$ model for each area vs. BSA_H averaged 0.99 (range of 0.974 to 1.023) and in no case was significantly different from 1. For the areas, each intercept *P* (the probability that the intercept is different from zero) was not significant (Table 3). Thus the nonzero intercept of the regressions for mitral, tricuspid, and pulmonary venous diameters vs. the zero intercept of the regressions of the mitral, tricuspid, and total pulmonary vein areas could be explained by BSA-dependent differences in relative size of the diameters and by the change in shape of those structures with growth.

Table 1. *Descriptive statistics for population age, body size, and cardiovascular parameters*

Parameter	*N*	Max	Min	Median	Mean	SD
Age, yr	496	20.00	0.00	4.47	5.94	5.52
Height, cm	496	188.4	45.5	104.3	107.6	38.2
Weight, kg	496	87.0	2.10	17.2	24.1	19.5
BSA_D, m^2	496	2.09	0.16	0.70	0.82	0.49
BSA_W, m^2	496	1.96	0.16	0.67	0.78	0.43
BSA_{Bw}, m^2	496	2.14	0.16	0.72	0.84	0.47
BSA_{Bhw}, m^2	496	2.11	0.16	0.73	0.84	0.47
BSA_H, m^2	496	2.11	0.16	0.72	0.83	0.48
AVA, cm	258	2.40	0.56	1.29	1.35	0.42
AoRt, cm	208	3.30	0.76	1.72	1.77	0.55
STJ, cm	161	2.80	0.66	1.44	1.49	0.49
TrAo, cm	146	2.51	0.54	1.11	1.22	0.42
AoIs, cm	147	2.05	0.46	1.01	1.05	0.34
LSCA, cm	68	0.90	0.20	0.50	0.54	0.18
LCA, cm	58	0.93	0.24	0.55	0.56	0.17
MV4C, cm	332	3.52	0.00	1.80	1.13	1.05
MV2C, cm	312	3.31	0.00	1.68	1.08	0.96
MVA, cm^2	118	8.55	0.67	2.53	2.99	1.76
TV4C, cm	125	3.40	0.79	1.70	1.81	0.58
TV2C, cm	127	3.56	0.85	1.87	1.91	0.59
TVA, cm^2	42	8.36	0.72	2.57	3.13	1.93
PVA, cm	140	2.30	0.64	1.20	1.29	0.41
MPA, cm	147	2.59	0.70	1.26	1.36	0.43
LPA, cm	166	1.65	0.34	0.83	0.87	0.28
RPA, cm	188	1.76	0.35	0.83	0.89	0.29
LLPV, cm	126	1.10	0.22	0.56	0.59	0.20
LUPV, cm	124	1.40	0.16	0.58	0.63	0.26
RLPV, cm	81	1.19	0.21	0.61	0.65	0.22
RUPV, cm	81	1.24	0.22	0.61	0.65	0.26
2DEDV, ml	149	199	5.10	40.1	50.0	37.1
HR, beats/mm	290	154	43	85.1	88.7	25.3
EDD, cm	290	5.99	1.73	3.57	3.59	1.00
$MMEDV_c$, ml	172	215	5.18	45.3	57.3	44.0
$MMEDV_{al}$, ml	172	208	6.35	43.6	58.3	42.9

2DEDV, 2-dimensional left ventricular end-diastolic volume; AVA, aortic valve annulus; AoRt, aortic root; BSA_D, body surface area calculated according to Du Bois and Du Bois formula; BSA_W, body surface area calculated according to Dreyer and Rey formula; BSA_{Bw}, body surface area calculated according to Boyd weight-based formula; BSA_{Bhw}, body surface area calculated according to Boyd height- and weight-based formula; BSA_H, body surface area calculated according to Haycock formula; EDD, left ventricular end-diastolic diameter; HR, heart rate; AoIs, aortic isthmus; LLPV, left lower pulmonary vein; LPA, left pulmonary artery; LCA, left carotid artery; LSCA, left subclavian artery; LUPV, left upper pulmonary vein; Max, maximum; Min, minimum; $MMEDV_{al}$, left ventricular diastolic volume derived from m-mode (area-length formula); $MMEDV_c$, left ventricular diastolic volume derived from m-mode (cubic formula); MPA, main pulmonary artery; MV4C, lateral dimension of mitral valve; MV2C, anteroposterior dimension of mitral valve; MVA, mitral valve area; *N,* number of observations; PVA, pulmonary anulus diameter; RLPV, right lower pulmonary vein; RPA, right pulmonary artery; RUPV, right upper pulmonary vein; SD, standard deviation; STJ, sinotubular junction of the ascending aorta; TrAo, distal transverse aortic diameter; TV4C, lateral dimension of tricuspid valve; TV2C, anteroposterior dimension of tricuspid valve; TVA, tricuspid valve area.

Indexed valvar and vascular dimensions and areas. The model that best described the data in a statistical sense was therefore a linear model with zero intercept ($Y = aX$) where $X = (BSA_H)^{0.5}$ for vascular and valvar dimensions and $X = BSA_H$ for vascular and valvar areas. On the basis of this finding, the adequacy of adjusting vessel and valvar dimensions by simple division by $(BSA_H)^{0.5}$ and of adjusting vessel and valvar areas by simple division by BSA_H was tested. As discussed above, if the effect of body size has been fully accounted for, the adjusted variable should have a distribution independent of body size. Indexed dimensions (D) were calculated as $D_I = D/(BSA_H)^{0.5}$ and indexed areas (A) were calculated as $A_I = A/BSA_H$. For each indexed variable, the regression vs. BSA_H was evaluated. The correlation coefficients and P values for these regressions are presented in Tables 2 and 3. With the exception of the mitral, tricuspid, and pulmonary vein dimensions, in each case the correlation was not significant, indicating that this method of indexing adequately accounts for the variance of the dimensions and areas with respect to BSA_H. The residual variance apparent in the indexed mitral and tricuspid dimensions was related to a BSA_H dependence of the magnitude of noncircularity of the valve orifice, with larger individuals tending to have more elliptical valves, although this relationship did not achieve statistical significance. This effect was eliminated when valve area was considered because there was no significant residual variance of the indexed valve areas with respect to BSA_H. Similarly, the significant residual variance in the indexed pulmonary vein dimensions was related to a BSA_H dependent variation in the relative size of the pulmonary veins, with larger subjects tending to have larger upper pulmonary veins compared with the lower veins. Again, when indexed TPVCSA was examined, there was no significant relation to BSA_H. The superiority of areas in accounting for the effect of BSA_H is the anticipated outcome if it is correct that total flow is the primary determinant of vascular and valvar size.

We tested for nonconstant variance (heteroscedasticity) of the relationship between indexed values vs. BSA_H by testing for skewness in the square of the residuals. The significance of this skewness is presented for each regression in Tables 2 and 3 (variance P). With the exception of the mitral and tricuspid lateral diameters, the magnitude of skewness was not statistically significant, indicating that this method of indexing adequately accounts for the effects of body size from a statistical point of view. Again, when mitral and tricuspid areas rather than diameters were considered there was no significant skewness to the residuals (Table 3), reflecting the same pattern as was noted for the issues of a significantly nonzero intercept and significant residual variance of the normalized variable vs. BSA_H. As with normal data obtained by others (1, 17, 23, 34, 38), the scatter of data points about the regression line tended to be greater for larger subjects as illustrated in Fig. 5*B*, an effect that is reduced but not completely eliminated by this method of indexing (Fig. 5*D*). However, because the nonconstant variance did not achieve statistically significant levels, estimation of the regression parameters remains unbiased (46).

Relation of left ventricular dimension and volume to body size. A predictive model of the relationship between left ventricular volume and body size was developed from the fact that CO is equal to the product of heart rate (HR), end-diastolic volume, and ejection fraction (EF), that is, CO = HR·EF·EDV. Combining the known linear relationship between CO and BSA [that is, $CO \approx BSA^{1.0}$ (22, 36)] with our findings that $HR \approx BSA^{-0.4}$ (Table 4) and that EF is independent of BSA, the predicted relationship is $EDV \approx BSA^{1.4}$. This prediction was evaluated against the observed data by analyzing the relationship between age, height, weight, and BSA as independent variables against left ventricular diastolic dimension and volume derived from two-dimensional echo and from m-mode echo (EDD, 2DEDV, $MMEDV_c$, and $MMEDV_{al}$). The results of this analysis are presented in Table 4. As was the case for

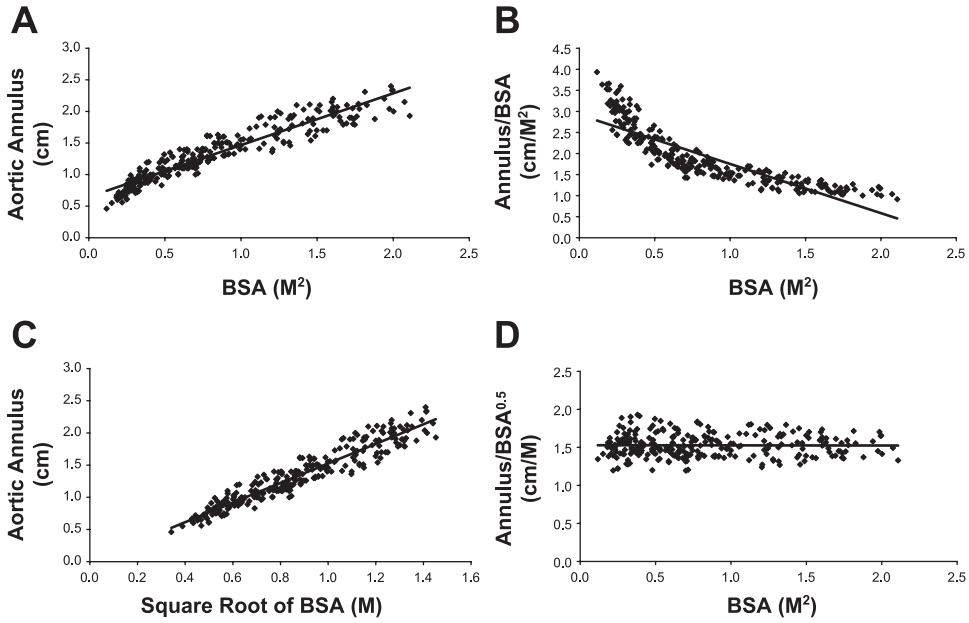

Fig. 5. Example of the inadequacy of "indexing" aortic valve annulus diameter to BSA. *A*: scatterplot of the relation between aortic annulus and BSA is shown along with the linear regression line. *B*: aortic annulus indexed to BSA (Annulus/BSA) is plotted against BSA. There is a highly significant correlation between Annulus/BSA and BSA, indicating that this method of indexing does not adequately account for the dependence of annulus size on BSA. *C*: relationship between aortic annulus and $BSA^{0.5}$. The regression is highly linear, and visual comparison with *A* indicates only subtle differences between the 2 regressions. Nevertheless, as shown in *D*, aortic annulus indexed by division by $BSA^{0.5}$ has no significant residual correlation with BSA, indicating that this method of indexing fully accounts for the variance of aortic annulus relative to BSA. BSA was calculated by the Haycock formula (27).

the vascular and valvar measurements, the best predictive equations with the highest R value and the lowest residual mean square were obtained with BSA_H compared with the other four methods of calculating BSA. The three-parameter model that included a nonzero intercept ($Y = aX^b + c$) did not significantly reduce explained variance, justifying use of the simpler two-parameter model ($Y = aX^b$). Left ventricular dimension related most closely to BSA^b with $b = 0.43$, whereas EDV, determined by the several different methods, related to BSA^b where mean $b = 1.38$ (range 1.343–1.398). This value is not significantly different from the predicted value of 1.4, confirming the validity of the predictive model.

DISCUSSION

Vascular and valvar dimensions. On the basis of statistical analysis, BSA was a more important determinant of the size of each of the 19 valvar and vascular dimensions studied in 496 normal children than either height or weight alone. In addition, of the several methods of calculating BSA that are in common use, the Haycock method was superior for describing the growth of cardiovascular structures. All vascular and valve diameters were linearly related to the square root of BSA whereas valvar and vascular areas were related to BSA. Some previous studies, as summarized in Table 5, reached similar conclusions. If this order dependence of the relationship between cardiovascular pathway dimension and body size dimension is ignored by simply indexing all variables to BSA, the indexed values have significant residual dependence on body size. More complex models such as polynomial regression, variable exponents, or variable intercepts do not describe the data more effectively. As in previous observations (25, 31, 34, 37, 50, 59, 68, 73), the intercepts of the regressions of vascular and valvar dimensions were zero or not significantly different from zero, allowing normal valvar and vascular diameters to be represented accurately by values indexed to $BSA^{0.5}$. Similarly, valvar and vascular areas were represented accurately by values indexed to BSA.

This analysis also illustrates how the method of calculation of BSA can affect the results, particularly in small children. The potential influence of the method of BSA calculation has been given insufficient attention, as reflected by the failure of most papers to even reference which method was used (Table 6). Caution is clearly needed when analyzing outcome on the basis of dimensions of a pathway if the normal values have been obtained by use of a different modality or measurement technique. For example, because the aortic and pulmonary artery areas vary by 9–12% (39) and TVA changes by a mean value of 26% during the cardiac cycle (53), use of autopsy values to derive a normal range for comparison of angiographic (2) or echocardiographic values is unlikely to be valid. This issue is emphasized by the large differences in the "normal" Nakata index (RPA + LPA area) (50) derived by different imaging techniques (Table 6). One of the strengths of this study is a uniform approach to the method of measurement and the inclusion of measurement of a large number of different structures obtained in the same laboratory. As a consequence, the variation in the derived exponent between the variables included in this study was significantly less than the variation between the studies summarized in Table 5.

We observed, as have others (1, 17, 23, 34, 38), that data spread tended to increase directly as a function of BSA. This nonconstant variance was reduced but not completely eliminated when dimensions were indexed by division by $BSA^{0.5}$, as seen in Fig. 5*D*. If it is assumed that the variance is constant with respect to BSA_H, the resulting prediction intervals result in an excess number of cases being incorrectly classified as above or below 2 standard deviations from the normal mean value. As discussed by Abbott and Gutgesell (1), it is therefore desirable to employ methods that further reduce the trend toward nonconstant variance when constructing confidence and prediction intervals. These methods include multiple regression techniques (3), variance stabilizing transformations (1, 3, 35, 46, 87), and weighted least squares analysis (77). Such statistical methods, although improving the accuracy of pre-

Table 2. *Relationship between body size and valvar and vascular dimensions and areas*

	AVA	AoRt	STJ	TrAo	AoIs	LSCA	LCA	MV4C	MV2C	TV4C	TV2C
Power function ($y = ax^b$), zero intercept, vs. height											
Exponent (b)	0.809	0.824	0.834	0.866	0.729	0.807	0.695	0.770	0.775	0.748	0.756
Constant (a)	0.031	0.037	0.030	0.023	0.036	0.013	0.022	0.052	0.047	0.060	0.056
R value	0.941	0.928	0.934	0.918	0.855	0.814	0.781	0.880	0.886	0.891	0.892
Resid MS	0.020	0.042	0.030	0.028	0.031	0.011	0.011	0.087	0.063	0.072	0.073
Power function ($y = ax^b$), zero intercept, vs. weight											
Exponent (b)	0.348	0.351	0.356	0.366	0.325	0.382	0.324	0.327	0.328	0.327	0.339
Constant (a)	0.475	0.617	0.513	0.439	0.413	0.181	0.214	0.711	0.654	0.748	0.727
R value	0.946	0.926	0.933	0.920	0.875	0.850	0.806	0.890	0.887	0.896	0.896
Resid MS	0.019	0.044	0.031	0.027	0.029	0.009	0.010	0.081	0.063	0.068	0.071
Power function ($y = ax^b$), zero intercept, vs. BSA_H											
Exponent (b)	0.494	0.500	0.507	0.502	0.459	0.528	0.455	0.472	0.474	0.461	0.468
Constant (a)	1.526	2.001	1.693	1.501	1.227	0.648	0.632	2.132	1.966	2.236	2.188
R value	0.948	0.930	0.936	0.925	0.878	0.855	0.810	0.894	0.890	0.899	0.899
Resid MS	0.017	0.040	0.029	0.025	0.027	0.008	0.008	0.079	0.061	0.066	0.069
Linear function ($y = ax + b$), vs. $(BSA_H)^{0.5}$											
Slope (a)	1.510	2.003	1.723	1.533	1.134	0.674	0.584	2.002	1.844	2.075	2.044
Intercept (b)	0.015	−0.002	−0.029	−0.032	0.089	−0.025	0.047	0.125	0.117	0.155	0.139
R value	0.948	0.929	0.937	0.924	0.876	0.853	0.809	0.890	0.891	0.897	0.898
Resid MS	0.017	0.041	0.029	0.025	0.028	0.008	0.009	0.081	0.062	0.067	0.069
Intercept P	0.602	0.961	0.537	0.478	0.155	0.578	0.376	0.068	0.068	0.047	0.088
Linear function with zero intercept ($y = ax$), vs. $(BSA_H)^{0.5}$											
Slope (a)	1.525	2.001	1.693	1.497	1.231	0.645	0.634	2.131	1.965	2.252	2.191
R value	0.948	0.929	0.937	0.924	0.871	0.850	0.805	0.888	0.889	0.896	0.896
Resid MS	0.017	0.041	0.029	0.025	0.028	0.009	0.010	0.082	0.062	0.068	0.070
Linear regression of $y/(BSA_H)^{0.5}$ vs. BSA_H											
R value	0.031	0.008	0.066	0.021	0.175	0.055	0.110	0.155	0.158	0.171	0.173
P value	0.625	0.910	0.408	0.799	0.040	0.654	0.412	0.030	0.029	0.056	0.052
Variance P	0.220	0.642	0.544	0.185	0.502	0.141	0.268	0.004	0.454	0.003	0.678

	PVA	MPA	RPA	LPA	LUPV	LLPV	RUPV	RLPV	AVG	MIN	MAX
Power function ($y = ax^b$), zero intercept, vs. height											
Exponent (b)	0.829	0.783	0.795	0.753	0.911	0.670	0.912	0.790	0.792	0.670	0.912
Constant (a)	0.031	0.038	0.023	0.027	0.009	0.027	0.010	0.017			
R value	0.927	0.905	0.896	0.880	0.797	0.755	0.864	0.866	0.874	0.755	0.941
Resid MS	0.024	0.034	0.017	0.018	0.025	0.016	0.017	0.016			
Power function ($y = ax^b$), zero intercept, vs. weight											
Exponent (b)	0.376	0.349	0.340	0.322	0.410	0.302	0.418	0.361	0.350	0.302	0.418
Constant (a)	0.492	0.524	0.340	0.347	0.195	0.255	0.197	0.233			
R value	0.920	0.899	0.891	0.869	0.804	0.764	0.876	0.868	0.880	0.764	0.946
Resid MS	0.027	0.036	0.018	0.020	0.024	0.016	0.016	0.012			
Power function ($y = ax^b$), zero intercept, vs. BSA_H											
Exponent (b)	0.520	0.490	0.483	0.488	0.577	0.424	0.584	0.505	0.495	0.424	0.584
Constant (a)	1.732	1.688	1.064	1.024	0.577	0.702	0.797	0.781			
R value	0.930	0.909	0.899	0.895	0.809	0.769	0.880	0.875	0.885	0.769	0.948
Resid MS	0.023	0.033	0.016	0.017	0.023	0.015	0.015	0.011			
Linear function ($y = ax + b$), vs. $(BSA_H)^{0.5}$											
Slope (a)	1.799	1.653	0.958	1.041	0.873	0.615	0.908	0.792			
Intercept (b)	−0.067	0.033	0.065	0.023	−0.098	0.084	−0.108	−0.011			
R value	0.929	0.908	0.897	0.896	0.806	0.764	0.878	0.872	0.889	0.764	0.948
Resid MS	0.024	0.033	0.017	0.017	0.024	0.016	0.015	0.012			
Intercept P	0.179	0.546	0.489	0.178	0.053	0.036	0.030	0.803			
Linear function with zero intercept ($y = ax$), vs. $(BSA_H)^{0.5}$											
Slope (a)	1.717	1.691	1.066	1.028	0.764	0.710	0.789	0.780			
R value	0.926	0.906	0.896	0.881	0.800	0.754	0.868	0.871	0.881	0.754	0.948
Resid MS	0.024	0.034	0.017	0.018	0.024	0.017	0.016	0.012			
Linear regression of $y/(BSA_H)^{0.5}$ vs. BSA_H											
R value	0.105	0.060	0.029	0.116	0.196	0.174	0.249	0.035	0.101	0.008	0.249
P value	0.217	0.468	0.697	0.137	0.029	0.051	0.025	0.755			
Variance P	0.837	0.687	0.445	0.278	0.160	0.106	0.103	0.341			

AVG, average value for parameter for all variables; Intercept P, significance of the difference of the intercept from zero; MAX, maximum value for parameter for all variables; MIN, minimum value for parameter for all variables; P value, significance of the correlation between each indexed variable and BSA_H; R value, correlation coefficient; Resid MS, regression residual mean square; S(%), mean percentage error of the estimate; Variance P, significance of the presence of heteroscedasticity in the regression.

Table 3. *Relationship between body size and valve and pulmonary vein areas*

	MVA	TVA	TPVCSA	AVG	MIN	MAX
Power function ($y = ax^b$), zero intercept, vs. height						
Exponent (b)	1.301	1.219	1.326	1.282	1.219	1.326
Constant (a)	0.007	0.014	0.003			
R value	0.897	0.938	0.842	0.892	0.842	0.938
Resid MS	0.622	0.491	0.273			
Power function ($y = ax^b$), zero intercept, vs. weight						
Exponent (b)	0.651	0.645	0.731	0.676	0.645	0.731
Constant (a)	0.367	0.454	0.162			
R value	0.897	0.942	0.846	0.895	0.846	0.942
Resid MS	0.615	0.424	0.261			
Power function ($y = ax^b$), zero intercept, vs. BSA_H						
Exponent (b)	0.979	0.984	1.020	0.994	0.979	1.020
Constant (a)	3.255	3.938	1.861			
R value	0.901	0.947	0.850	0.899	0.850	0.947
Resid MS	0.593	0.405	0.259			
Linear function ($y = ax + b$), vs. BSA_H						
Slope (a)	3.091	3.661	1.922			
Intercept (b)	0.140	0.236	−0.056			
R value	0.901	0.947	0.850	0.899	0.850	0.947
Resid MS	0.594	0.405	0.258			
Intercept P	0.341	0.206	0.698			
Linear function with zero intercept ($y = ax$), vs. BSA_H						
Slope (a)	3.207	3.875	1.864			
R value	0.900	0.946	0.850	0.899	0.850	0.947
Resid MS	0.599	0.411	0.259			
Linear regression of y/BSA_H vs. BSA_H						
R value	0.105	0.156	0.091	0.117	0.091	0.156
P value	0.124	0.102	0.532			
Variance P	0.673	0.490	0.870			

TPVCSA, total pulmonary vein cross-sectional area.

diction intervals, are invariably ad hoc and lack a sound physiological basis on which to base the choice of one method over another. In the present analysis, we were primarily attempting to understand the relationship between body size and growth of cardiovascular structures. For this purpose, the observation that the nonconstant variance did not achieve statistical significance was sufficient to ensure unbiased estimates of the regression parameters (46).

The $Y = aX^b$ model of vascular and valve development with growth was predicted theoretically and confirmed empirically. The findings support a causal relationship because the observed measurements and the cardiovascular dimensions adjusted for body size according to the proposed model are similar to the values predicted by the theoretical analysis based on the principle of minimum work. Besides the validation of the analysis of the cardiovascular pathway dimensions vs. body

Table 4. *Relationship between parameters of body size and heart rate, ventricular dimensions, and volumes*

	2DEDV	HR	EDD	$MMEDV_c$	$MMEDV_{al}$
Power function ($y = ax^b$), zero intercept, vs. height					
Exponent (b)	1.996	−0.643	0.709	2.204	1.608
Constant (a)	0.005	1753	0.128	0.001	0.027
R value	0.917	0.881	0.950	0.935	0.923
Resid MS	262.5	172.5	0.098	247.1	262.3
Power function ($y = ax^b$), zero intercept, vs. weight					
Exponent (b)	0.893	−0.283	0.307	0.899	0.892
Constant (a)	3.480	208.0	1.397	3.036	3.140
R value	0.923	0.877	0.944	0.926	0.937
Resid MS	244.9	178.1	0.108	279.4	225.8
Power function ($y = ax^b$), zero intercept, vs. BSA_H					
Exponent (b)	1.385	−0.402	0.444	1.398	1.343
Constant (a)	69.71	80.33	3.935	61.66	62.40
R value	0.924	0.882	0.961	0.944	0.966
Resid MS	242.3	171.4	0.076	211.1	125.3
Power function ($y = ax^b + c$), variable intercept, vs. BSA_H					
Exponent (b)	1.169	−0.401	0.371	1.416	1.345
Intercept (c)	−4.797	3.199	−0.703	3.102	0.541
Constant (a)	75.47	77.127	4.657	57.81	61.75
R value	0.924	0.881	0.961	0.945	0.966
Resid MS	243.2	173.3	0.076	211.3	126.0

Table 5. *Nature of the relationships between cardiac dimensions and body size as reported in the literature*

Modality	Reference	Structures Studied	*n*	Index	Exponential Growth Model	Exponent	Nonconstant Variance
Valves and vessels							
Autopsy	81	MPA,RPA,LPA	126	d/Ht			No
Autopsy	80	AVA,AsAo,AoIs,PVA,MPA,RPA,LPA	126	d/Ht			No
Angio	68	AVA,AsAo,PVA,MPA,RPA,LPA	24		BSA	0.47–0.58	Yes
Angio	25	AVA,MPA,RPA,LPA	35		BSA	0.45–0.69	No
Angio	50	RPA,LPA	40	a/BSA			Yes
2DEcho	31	MPA,AsAo	173	$d/BSA^{0.5}$	BSA	0.5	No
2DEcho	73	AsAo,TrAo,RPA,MPA	110		BSA	0.5	Yes
2DEcho	25	AVA,AsAo,RPA	7	$d/BSA^{0.5}$			No
2DEcho	23	AVA,PVA	70	a/BSA	BSA	0.5	Yes
2DEcho	61	AVA	187	a/BSA			No
2DEcho	13	AVA	36	a/BSA			No
2DEcho	70	AVA,PVA	36	a/BSA			No
2DEcho	37	RPA	50	$d/BSA^{0.5}$	BSA	0.51–0.52	No
2DEcho	57	MVA	20	a/BSA			No
2DEcho	59	MVA	50	a/BSA			No
2DEcho	Personal	19 valve or vessel diameters	496	$d/BSA^{0.5}$	BSA	0.45–0.52	Yes
Left ventricular volume and mass							
Angio	25	RVV,LVV	819		BSA	1.34–1.52	No
Angio	36	RVV,LVV	105		BSA	1.17–1.34	Yes
Angio	51	LVV	24		BSA	1.3	No
2DEcho	25	LVM,LVV	7	$v/BSA^{1.5}$			No
2DEcho	14	LVM	611	$v/BSA^{1.5}$	BSA	1.3–1.6	Yes
Conduct	29	LVV	10	v/Wt			
2DEcho	Personal	LVV	496		BSA	1.27–1.36	Yes
Left ventricular diameter							
2DEcho	55	EDD	268		BSA	0.42–0.48	Yes
2DEcho	28	EDD	105		BSA	0.5	Yes
2DEcho	24	EDD	145		Ht,Wt,BSA	0.33–0.5	No
2DEcho	25	EDD	819		BSA	0.36–0.51	Yes
2DEcho	38	EDD	202		BSA	0.41–0.44	No
2DEcho	Personal	EDD	256		BSA	0.43	Yes

a, Area; AsAo, ascending aorta; Angio, angiography; 2DEcho, 2-dimensional echocardiography; Conduct, conductance catheter; Personal, present study; d, diameter; Ht, height; LVM, left ventricular mass; LVV, left ventricular volume; *n,* number of subjects; RVV, right ventricular volume; Wt, weight; v, volume.

size relation, the data support the hypothesis that cardiac and vascular pathways adapt to peak levels of pressure and volume demand. The diameters observed are optimal in terms of energy dissipation for CO equivalent to two times resting CO in infants and three to four times resting CO in older children. These findings are similar to the comparison between observed and theoretically predicted coronary size on the basis of the minimal work principle (66).

Ventricular dimensions and volumes. In accord with some previous studies (14), we found BSA to be a more important determinant of left ventricular dimension and volume in normal subjects than age, height, or weight alone. Unlike the linear relation of valve and vessel diameters to the square root of BSA, the effect of body size on left ventricular dimensions was not fully accounted for by adjustments for the square root of BSA. Similarly, contrary to the predicted relationship of volume relating to $weight^{1.0}$ and to $BSA^{1.5}$, ventricular size has a more complex relation with body size. In contrast to vascular and vessel growth, which depend directly on CO, the relationship between ventricular size and CO also depends on heart rate such that ventricular diastolic volume would only be predicted to relate to $BSA^{1.5}$ if heart rate were a function of $BSA^{-0.5}$. In this study, we found that the relationship between heart rate and BSA had an exponent of −0.4, that is $HR = aBSA^{-0.4}$. Similar observations ($HR = a'BSA^{-0.38}$) were made in series of different species of mammals with a 1,800- to 500,000-fold increase of body weight (29, 60). The increasing resistance to blood flow and the power output available from the heart muscle with increasing body size are the limiting factors of the frequency of the heart beat, as derived mathematically and shown by the measured data available (74). Because of the inverse relation of heart rate with BSA and of the linear relation between CO and BSA (22, 36), left ventricular volume was more closely related to $BSA^{1.4}$ as observed in the subjects of this study and in the literature (Table 5) than to $BSA^{1.5}$. Similar to our findings, left ventricular diameters have been most closely related to $BSA^{0.4-0.45}$ (Table 5). It is also clear that when factors other than BSA influence basal heart rate, the relationship between BSA and ventricular size can be expected to change. Two well-known examples of this are complete heart block and training-induced bradycardia, both of which are associated with ventricular volumes larger than would be predicted for BSA. Less well investigated and outside of the scope of this study is whether the normal age-related fall in heart rate in adults similarly influences the relationship between heart rate and ventricular size, creating a need for indexing ventricular size for both age and BSA.

Limitations of the study. A potential limitation of this study is that the optimal dimensions derived from the principle of minimal work were based on the assumption that CO is linearly related to BSA. The results of various investigations into the variance between CO and BSA have varied from a first order linear relationship (22, 36) to a 0.6 power relationship (29), but

Table 6. *Reported normalized dimensions of cardiac pathways in normal individuals*

Modality	Method	Reference	Subjects	Time in Cycle	BSA Method	BSA Range	Area/BSA, cm^2/m^2	Diameter/$BSA^{0.5}$, cm/m
Mitral valve								
Autopsy	CIRC	64	C		BSA_D	0.2–1.8	3.4	2.0
Autopsy	CIRC	83	A		NS	1.2–2.8	4.3	2.3
2DEcho	IN-IN	Personal	C	Max	BSA_H	0.2–2.0	3.3	2.2
2DEcho	Area	53	A	Max	NS	NS	3.8	2.2
2DEcho	Area	57	A	Max	NS	NS	4.2	2.3
2DEcho	Area	59	C	Max	BSA_D	0.2–0.9	4.7	2.4
2DEcho	IN-IN	34	C	Max	NS	0.2–1.4	3.3	2.0
Tricuspid valve								
Autopsy	CIRC	64	C		BSA_D	0.2–1.8	4.5	2.4
Autopsy	CIRC	83	A		NS	1.2–2.8	5.8	2.7
2DEcho	IN-IN	Personal	C	Max	BSA_H	0.2–2.0	4.0	2.2
2DEcho	IN-IN	34	C	Max	NS	0.2–1.4	3.8	2.2
2DEcho	Area	76	A	Max	NS	NS	6.1	2.8
Aortic annulus								
Autopsy	CIRC	64	C		BSA_D	0.2–1.8	1.6	1.4
Autopsy	CIRC	83	A		NS	1.2–2.8	2.4	1.7
Angio	IN-IN	68	C	Max, Min	NS	0.2–1.5	2.9	1.9
2DEcho	IN-IN	Personal	C	Max	BSA_H	0.2–2.0	1.8	1.5
2DEcho	IN-IN	26	C	NS	NS	0.2–1.6	2.4	1.7
2DEcho	Area	57	A	Max	NS	NS	1.8	1.5
Doppler	CONT	70	A		NS	1.1–2.0	1.8	1.5
Doppler	CONT	23	C		NS	0.1–2.1	1.3	1.3
Pulmonary annulus								
Autopsy	CIRC	64	C		BSA_D	0.2–1.8	1.9	1.6
Autopsy	CIRC	83	A		NS	1.2–2.8	2.6	1.8
Angio	IN-IN	68	C	Max,Min	NS	0.2–1.5	2.8	1.9
Angio	IN-IN	35	C	Max,Min	NS	NS	2.8	1.9
2DEcho	IN-IN	Personal	C	Max	BSA_H	0.2–2.0	2.3	1.7
2DEcho	IN-IN	26	C	NS	NS	0.2–1.6	2.8	1.9
Doppler	CONT	70	A		NS	1.1–2.0	2.0	1.6
Doppler	CONT	23	C		NS	0.1–2.1	1.7	1.5
Main pulmonary artery								
Angio	IN-IN	68	C	Max,Min	NS	0.2–1.5	3.5	2.1
Angio	IN-IN	35	C	Max,Min	NS	NS	3.5	2.1
2DEcho	IN-IN	Personal	C	Max	BSA_H	0.2–2.0	2.3	1.7
2DEcho	OUT-IN	73	C	ES,ED	BSA_D	0.2–2.0	2.2	1.5
Right pulmonary artery								
Angio	IN-IN	68	C	Max,Min	NS	0.2–1.5	1.8	1.5
Angio	IN-IN	35	C	Max,Min	NS	NS	1.8	1.5
2DEcho	IN-IN	Personal	C	Max	BSA_H	0.2–2.0	0.9	1.1
2DEcho	OUT-IN	37	C	ES,ED	BSA_D	0.2–1.8	1.6	1.4
2DEcho	OUT-IN	73	C	ES,ED	BSA_D	0.2–2.0	1.1	1.2
Left pulmonary artery								
Angio	IN-IN	68	C	Max,Min	NS	0.2–1.5	1.6	1.4
Angio	IN-IN	35	C	Max,Min	NS	NS	1.4	1.3
2DEcho	IN-IN	Personal	C	Max	BSA_H	0.2–2.0	0.9	1.0
Sum of right and left pulmonary artery								
Angio	IN-IN	68	C	Max,Min	NS	0.2–1.5	3.4	2.9
Angio	IN-IN	35	C	Max,Min	NS	NS	3.2	2.8
Angio	IN-IN	50	C	Mean	NS	0.3–1.6	3.3	2.9
2DEcho	IN-IN	Personal	C	Max	BSA_H	0.2–2.0	1.9	2.1

2DEcho, 2-dimensional echocardiography; A, Adults; Angio, angiography; BSA_D, Dubois and Dubois formula for body surface area; BSA_H, Haycock formula for body surface area; C, Children; CIRC, circumference; CONT, Continuity equation; IN-IN, inner edge to inner edge measurement; Max, maximum; Min, minimum; OUT-IN, outer (leading) edge to inner edge measurement; Time in cycle, time during the cardiac cycle at which the measurement was taken (not applicable for autopsy- or Doppler-derived values); NS, not stated.

in humans the relationship has been found to be linear. The hypothesis that the relation between CO and BSA is linear is also supported by the observation that the relation between the dimensions of transverse aorta and its branches, which are linearly related to BSA, obeys the theoretical principle of optimum dimension relation that underlies vascular tree structure, and is calculated independently of CO values.

In conclusion, in children, BSA is a more important determinant of the size of each cardiac or vascular structure than height or weight alone. The method of calculation of BSA is also important, with the Haycock formula providing the best estimate with regard to the growth of cardiovascular structures. Cardiac and vascular pathway diameters vary linearly with the square root of BSA and valve and vascular areas vary linearly with BSA. Because the intercept of the regression is zero, the valve and vascular diameters are represented accurately by the values indexed for the square root of BSA by division. The distribution around the mean value of the index allows for an

accurate representation of normals without the bias of heteroscedasticity and skewness in predictions using linear regression and ordinary or weighted least squares (1). Residual analysis showed that the effect of body size has been fully accounted for by demonstrating the independence of the index of valve and vascular dimensions and of the residuals with body size. Values derived from the theoretical principles of minimal work and the principles underlying vascular tree structure are similar to the observed measurements and to the dimensions adjusted for body size according to the proposed model. Aside from the validation of the analysis of cardiovascular dimension-body size relation, it supports the concept that cardiac and vascular pathways adapt to peak or mean 24 h level of CO. In contrast, because of a nonlinear decrease of heart rate with growth, the effects of body size on left ventricular size were not fully accounted for by similar adjustment for proportional powers of BSA, with ventricular volumes proportional to weight$^{0.9}$ and BSA$^{1.4}$. The underlying relationship between BSA and CO does indeed appear to be the fundamental control mechanism that influences the growth of vessel and chamber size, but the variability of heart rate with body size adds an additional level of complexity to the control of chamber growth.

REFERENCES

1. **Abbott RD and Gutgesell HP.** Effects of heteroscedasticity and skewness on prediction in regression: modeling growth of the human heart. *Methods Enzymol* 240: 37–51, 1994.
2. **Alboliras ET, Julsrud PR, Danielson GK, Puga FJ, Schaff HV, McGoon DC, Hagler DJ, Edwards WD, and Driscoll DJ.** Definitive operation for pulmonary atresia with intact ventricular septum. Results in twenty patients. *J Thorac Cardiovasc Surg* 93: 454–464, 1987.
3. **Bates DM and Watts DG.** *Nonlinear Regression Analysis and Its Applications.* New York: Wiley, 1988.
4. **Binder RC.** *Fluid Mechanics.* Englewood Cliffs, NJ: Prentice-Hall, 1973.
5. **Blackstone EH, Kirklin JW, Bertranou EG, Labrosse CJ, Soto B, and Bargeron LM Jr.** Preoperative prediction from cineangiograms of post-repair right ventricular pressure in tetralogy of Fallot. *J Thorac Cardiovasc Surg* 78: 542–552, 1979.
6. **Blackstone EH, Kirklin JW, and Pacifico AD.** Decision-making in repair of tetralogy of Fallot based on intraoperative measurements of pulmonary arterial outflow tract. *J Thorac Cardiovasc Surg* 77: 526–532, 1979.
7. **Boyd E.** *The Growth of the Surface Area of the Human Body.* Westport, CT: Greenwood, 1935.
8. **Bruce RA.** Left ventricular dimensions and function in athletes: cardiac or cardiovascular adaptations, or both. *J Am Coll Cardiol* 15: 589–590, 1990.
9. **Calder AL, Barratt-Boyes BG, Brandt PW, and Neutze JM.** Postoperative evaluation of patients with tetralogy of Fallot repaired in infancy. Including criteria for use of outflow patching and radiologic assessment of pulmonary regurgitation. *J Thorac Cardiovasc Surg* 77: 704–720, 1979.
10. **Caro CC, Pedley TJ, Schroter RC, and Seed WA.** Flow in pipes and around objects. In: *The Mechanics of the Circulation*, edited by Caro CG, Pedley TJ, Schroter RC, and Seed WA. New York: Oxford University Press, 1978, p. 44–78.
11. **Colan SD, Parness IA, Spevak PJ, and Sanders SP.** Developmental modulation of myocardial mechanics: age- and growth-related alterations in afterload and contractility. *J Am Coll Cardiol* 19: 619–629, 1992.
12. **Colan SD, Sanders SP, and Borow KM.** Physiologic hypertrophy: effects on left ventricular systolic mechanics in athletes. *J Am Coll Cardiol* 9: 776–783, 1987.
13. **Davidson WR, Pasquale MJ, and Fanelli C.** A Doppler echocardiographic examination of the normal aortic valve and left ventricular outflow tract. *Am J Cardiol* 67: 547–549, 1991.
14. **De Simone G, Daniels SR, Devereux RB, Meyer RA, Roman MJ, De Divitiis O, and Alderman MH.** Left ventricular mass and body size in normotensive children and adults: assessment of allometric relations and impact of overweight. *J Am Coll Cardiol* 20: 1251–1260, 1992.
15. **Dreyer G and Ray W.** Further experiments upon the blood volume of mammals and its relation to the surface area of the body. *Philos Trans R Soc Lond* 202: 191–212, 1912.
16. **Du Bois D and Du Bois EF.** A formula to estimate the approximate surface area if height and weight be known. *Arch Intern Med* 17: 863–871, 1916.
17. **El Habbal M and Somerville J.** Size of the normal aortic root in normal subjects and in those with left ventricular outflow obstruction. *Am J Cardiol* 63: 322–326, 1989.
18. **Fisher AG, Adams TD, Yanowitz FG, Ridges JD, Orsmond G, and Nelson AG.** Noninvasive evaluation of world class athletes engaged in different modes of training. *Am J Cardiol* 63: 337–341, 1989.
19. **Fisman EZ, Frank AG, Ben-Ari E, Kessler G, Pines A, Drory Y, and Kellermann JJ.** Altered left ventricular volume and ejection fraction responses to supine dynamic exercise in athletes. *J Am Coll Cardiol* 15: 582–588, 1990.
20. **Fung YC.** Blood flow in arteries. In: *Biodynamics: Circulation*, edited by Fung YC. New York: Springer-Verlag, 1984, p. 77–165.
21. **Graham TP Jr, Jarmakani JM, Canent RV Jr and Morrow MN.** Left heart volume estimation in infancy and childhood. Reevaluation of methodology and normal values. *Circulation* 43: 895–904, 1971.
22. **Grollman A.** Physiologic variations in the cardiac output in man. *Am J Physiol* 90: 210–217, 1929.
23. **Gutgesell HP and French M.** Echocardiographic determination of aortic and pulmonary valve areas in subjects with normal hearts. *Am J Cardiol* 68: 773–776, 1991.
24. **Gutgesell HP, Paquet M, Duff DF, and McNamara DG.** Evaluation of left ventricular size and function by echocardiography. Results in normal children. *Circulation* 56: 457–462, 1977.
25. **Gutgesell HP and Rembold CM.** Growth of the human heart relative to body surface area. *Am J Cardiol* 65: 662–668, 1990.
26. **Hanseus K, Bjorkhem G, and Lundstrom NR.** Dimensions of cardiac chambers and great vessels by cross-sectional echocardiography in infants and children. *Pediatr Cardiol* 9: 7–16, 1988.
27. **Haycock GB, Schwartz GJ, and Wisotsky DH.** Geometric method for measuring body surface area: a height-weight formula validated in infants, children, and adults. *J Pediatr* 93: 62–66, 1978.
28. **Henry WL, Ware J, Gardin JM, Hepner SI, McKay J, and Weiner M.** Echocardiographic measurements in normal subjects. Growth-related changes that occur between infancy and early adulthood. *Circulation* 57: 278–284, 1978.
29. **Holt JP, Rhode EA, and Kines H.** Ventricular volumes and body weight in mammals. *Am J Physiol* 215: 704–715, 1968.
30. **Horsfield K.** Diameters, generation, and orders in the bronchial tree. *J Appl Physiol* 68: 457–461, 1990.
31. **Ichida F, Aubert A, Denef B, Dumoulin M, and Van der Hauwaert LG.** Cross sectional echocardiographic assessment of great artery diameters in infants and children. *Br Heart J* 58: 627–634, 1987.
32. **Kamiya A and Togawa T.** Optimal branching structures of the vascular tree. *Bull Math Biophys* 34: 431–438, 1972.
33. **Kamiya A and Togawa T.** Theoretical relationship between the optimal models of the vascular tree. *Bull Math Biophys* 36: 311–323, 1974.
34. **King DH, Smith EO, Huhta JC, and Gutgesell HP.** Mitral and tricuspid valve anular diameter in normal children determined by two-dimensional echocardiography. *Am J Cardiol* 55: 787–789, 1985.
35. **Kirklin JW, Blackstone EH, Jonas RA, and Kouchoukos NT.** Anatomy, dimensions, and terminology. In: *Cardiac Surgery*, edited by Kirklin JW and Barrat-Boyes BG. New York: Churchill Livingstone, 1993, p. 21–60.
36. **Lange PE, Onnasch DG, Schaupp GH, Zill C, and Heintzen PH.** Size and function of the human left and right ventricles during growth. Normative angiographic data. *Pediatr Cardiol* 3: 205–211, 1982.
37. **Lappen RS, Riggs TW, Lapin GD, Paul MH, and Muster AJ.** Two-dimensional echocardiographic measurement of right pulmonary artery diameter in infants and children. *J Am Coll Cardiol* 2: 121–126, 1983.
38. **Lester LA, Sodt PC, Hutcheon N, and Arcilla RA.** M-mode echocardiography in normal children and adolescents: some new perspectives. *Pediatr Cardiol* 8: 27–33, 1987.
39. **Loeber CP, Goldberg SJ, Marx GR, Carrier M, and Emery RW.** How much does aortic and pulmonary artery area vary during the cardiac cycle? *Am Heart J* 113: 95–100, 1987.
40. **Lyne WH.** Unsteady viscous flow in a curved pipe. *J Fluid Mech* 45: 13–22, 1971.

41. **Marquardt DW.** An algorithm for least-squares estimation of nonlinear parameters. *J Soc Ind Appl Math* 11: 431–441, 1963.
42. **Matitiau A, Geva T, Colan SD, Sluysmans T, Parness IA, Spevak PJ, van der Velde M, Mayer JE Jr, and Sanders SP.** Bulboventricular foramen size in infants with double-inlet left ventricle or tricuspid atresia with transposed great arteries: influence on initial palliative operation and rate of growth. *J Am Coll Cardiol* 19: 142–148, 1992.
43. **Milliken MC, Stray Gundersen J, Peshock RM, Katz J, and Mitchell JH.** Left ventricular mass as determined by magnetic resonance imaging in male endurance athletes. *Am J Cardiol* 62: 301–305, 1988.
44. **Milnor WR.** The normal hemodynamic state. In: *Hemodynamics*, edited by Milnor WR. Baltimore, MD: Williams & Wilkins, 1982, p. 135–156.
45. **Milnor WR.** Steady flow. In: *Hemodynamics*. Baltimore, MD: Williams & Wilkins, 1989, p. 11–50.
46. **Montgomery DC and Peck EA.** *Introduction to Linear Regression Analysis*. New York: Wiley, 1992.
47. **Murray CD.** The physiologic principle of minimal work applied to the angle of branching arteries. *J Gen Physiol* 6: 835–841, 1926.
48. **Murray CD.** The physiologic principle of minimum work: I. The vascular system and the cost of blood volume. *Proc Natl Acad Sci USA* 12: 207–214, 1926.
49. **Murray CD.** A relationship between circumference and weight in trees and its bearing on branching angles. *J Gen Physiol* 11: 431–441, 1927.
50. **Nakata S, Imai Y, Takanashi Y, Kurosawa H, Tezuka K, Nakazawa M, Ando M, and Takao A.** A new method for the quantitative standardization of cross-sectional areas of the pulmonary arteries in congenital heart diseases with decreased pulmonary blood flow. *J Thorac Cardiovasc Surg* 88: 610–619, 1984.
51. **Nomoto S, Muraoka R, Yokota M, Aoshima M, Kyoku I, and Nakano H.** Left ventricular volume as a predictor of postoperative hemodynamics and a criterion for total correction of tetralogy of Fallot. *J Thorac Cardiovasc Surg* 88: 389–394, 1984.
52. **Onnasch DG, Lange PE, and Heintzen PH.** Left ventricular muscle volume in children and young adults. *Pediatr Cardiol* 5: 101–106, 1984.
53. **Ormitson JA, Shah PM, Tei C, and Wong M.** Size and motion of the mitral valve annulus in man. I. A two-dimensional echocardiographic method and findings in normal subjects. *Circulation* 64: 113–120, 1981.
54. **Pacifico AD, Kirklin JW, and Blackstone EH.** Surgical management of pulmonary stenosis in tetralogy of Fallot. *J Thorac Cardiovasc Surg* 74: 382–395, 1977.
55. **Pearlman JD, Triulzi MO, King ME, Newell J, and Weyman AE.** Limits of normal left ventricular dimensions in growth and development: analysis of dimensions and variance in the two-dimensional echocardiograms of 268 normal healthy subjects. *J Am Coll Cardiol* 12: 1432–1441, 1988.
56. **Pollanen MS.** Dimensional optimization at different levels of the arterial hierarchy. *J Theor Biol* 159: 267–270, 1992.
57. **Pollick C, Pittman M, Filly K, Fitzgerald PJ, and Popp RL.** Mitral and aortic valve orifice area in normal subjects and in patients with congestive cardiomyopathy: determination by two dimensional echocardiography. *Am J Cardiol* 49: 1191–1196, 1982.
58. **Reichek N, Helak J, Plappert T, St John Sutton MG, and Weber KT.** Anatomic validation of left ventricular mass estimates from clinical two-dimensional echocardiography: initial results. *Circulation* 67: 348–352, 1983.
59. **Riggs TW, Lapin GD, Paul MH, Muster AJ, and Berry TE.** Measurement of mitral valve orifice area in infants and children by two-dimensional echocardiography. *J Am Coll Cardiol* 1: 873–878, 1983.
60. **Rihl J.** Die frequenz des herzschlages. In: *Handbuch der normalen und pathologischen physiologie*. Berlin: Springer, 1926, p. 449–457.
61. **Roman MJ, Devereux RB, Kramer-Fox R, and O'Loughlin J.** Two-dimensional echocardiographic aortic root dimensions in normal children and adults. *Am J Cardiol* 64: 507–512, 1989.
62. **Rossitti S and Frisen L.** Remodelling of the retinal arterioles in descending optic atrophy follows the principle of minimum work. *Acta Physiol Scand* 152: 333–340, 1994.
63. **Rossitti S and Löfgren J.** Vascular dimensions of the cerebral arteries follow the principle of minimum work. *Stroke* 24: 371–377, 1993.
64. **Rowlatt UF, Rimoldi HJA, and Lev M.** The quantitative anatomy of the normal heart. *Pediatr Clin North Am* 10: 499–588, 1963.
65. **Savage DD, Levy D, Dannenberg AL, Garrison RJ, and Castelli WP.** Association of echocardiographic left ventricular mass with body size, blood pressure and physical activity (the Framingham Study). *Am J Cardiol* 65: 371–376, 1990.
66. **Seiler C, Kirkeeide RL, and Gould KL.** Basic structure-function relations of the epicardial coronary vascular tree: basis of quantitative coronary arteriography for diffuse coronary artery disease. *Circulation* 85: 1987–2003, 1992.
67. **Sherman TF.** On connecting large vessels to small: the meaning of Murray's law. *J Gen Physiol* 78: 431–453, 1981.
68. **Sievers HH, Onnasch DG, Lange PE, Bernhard A, and Heintzen PH.** Dimensions of the great arteries, semilunar valve roots, and right ventricular outflow tract during growth: normative angiocardiographic data. *Pediatr Cardiol* 4: 189–196, 1983.
69. **Silverman NH, Ports TA, Snider AR, Schiller NB, Carlsson E, and Heilbron DC.** Determination of left ventricular volume in children: echocardiographic and angiographic comparisons. *Circulation* 62: 548–557, 1980.
70. **Singh B and Mohan JC.** Doppler echocardiographic determination of aortic and pulmonary valve orifice areas in normal adult subjects. *Int J Cardiol* 37: 73–78, 1992.
71. **Sluysmans T, Neven B, Rubay J, Lintermans J, Ovaert C, Mucumbitsi J, Shango P, Stijns M, and Vliers A.** Early balloon dilatation of the pulmonary valve in infants with tetralogy of Fallot: risks and benefits. *Circulation* 91: 1506–1511, 1995.
72. **Sluysmans T, Sanders SP, van der Velde M, Matitiau A, Parness IA, Spevak PJ, Mayer JE Jr, and Colan SD.** Natural history and patterns of recovery of contractile function in single left ventricle after Fontan operation. *Circulation* 86: 1753–1761, 1992.
73. **Snider AR, Enderlein MA, Teitel DF, and Juster RP.** Two-dimensional echocardiographic determination of aortic and pulmonary artery sizes from infancy to adulthood in normal subjects. *Am J Cardiol* 53: 218–224, 1984.
74. **Spatz HC.** Circulation, metabolic rate, and body size in mammals. *J Comp Physiol [B]* 161: 231–236, 1991.
75. **Tanner JM.** Fallacy of per-weight and per-surface area standards, and their relation to spurious correlation. *J Appl Physiol* 2: 1–15, 1949.
76. **Tei C, Pilgrim JP, Shah PM, Ormitson JA, and Wong M.** The tricuspid valve annulus: study of motion in normal subjects and in patients with tricuspid regurgitation. *Circulation* 66: 675–681, 1982.
77. **Theil H.** *Principles of Econometrics*. New York: Wiley, 1971.
78. **Thompson DW.** On the shape of eggs and certain other hollow structures. In: *On Growth and Form*. New York: Macmillan, 1943, p. 457–461.
79. **Uylings HBM.** Optimization of diametres and bifurcation angles in lungs and vascular tree structures. *Bull Math Biol* 39: 509–520, 1977.
80. **Van Meurs van Woezik H, Debets T, and Klein HW.** Internal diameters of the ventriculo-arterial junctions and great arteries of normal infants and children: a data base for evaluation of congenital cardiac malformations. *Int J Cardiol* 23: 303–308, 1989.
81. **Van Meurs van Woezik H, Debets T, and Klein HW.** Growth of the internal diameters in the pulmonary arterial tree in infants and children. *J Anat* 151: 107–115, 1987.
82. **Weibel ER.** *Morphometry of the Human Lung*. New York: Academic, 1963.
83. **Westaby S, Karp RB, Blackstone EH, and Bishop SP.** Adult human valve dimensions and their surgical significance. *Am J Cardiol* 53: 552–556, 1984.
84. **Wyatt HL, Heng MK, Meerbaum S, Gueret P, Hestenes J, Dula E, and Corday E.** Cross-sectional echocardiography. II. Analysis of mathematic models for quantifying volume of the formalin-fixed left ventricle. *Circulation* 61: 1119–1125, 1980.
85. **Yoganathan AP, Cape EG, Sung HW, Williams FP, and Jimoh A.** Review of hydrodynamic principles for the cardiologist: Applications to the study of blood flow and jets by imaging techniques. *J Am Coll Cardiol* 12: 1344–1353, 1988.
86. **Zamir M.** The role of shear forces in arterial branching. *J Gen Physiol* 67: 213–222, 1976.
87. **Zar JH.** *Biostatistical Analysis.* Englewood Cliffs, NJ: Prentice-Hall, 1974.